

# Measurements with a noninvasive detector and dephasing mechanism

S.A. Gurvitz

*Department of Particle Physics, Weizmann Institute of Science, Rehovot 76100, Israel*

(September 7, 2018)

## Abstract

We study dynamics of the measurement process in quantum dot systems, where a particular state out of coherent superposition is observed. The ballistic point-contact placed near one of the dots is taken as a noninvasive detector. We demonstrate that the measurement process is fully described by the Bloch-type equations applied to the whole system. These equations clearly reproduce the collapse of the density-matrix into the statistical mixture in the course of the measurement process. The corresponding dephasing width is uniquely defined. We show that the continuous observation of one of the states in a coherent superposition may *accelerate* decay from this state – in contradiction with rapidly repeated observations, which slow down the transitions between quantum states (the quantum Zeno effect).

## I. INTRODUCTION

In recent years there have been many measurements in mesoscopic systems sensitive to the phase of electronic wave function. We mention the experiments with double split systems [1,2], quantum dot embedded in Aharonov-Bohm ring [3,4], and coupled quantum dots [5]. It is known that the phase of wave function, or more precisely the off-diagonal density matrix

elements, can be destroyed by interaction with the environment or with the measurement device. As a result, the density matrix becomes the statistical mixture. The latter does not display any coherence effects. Now the rapid progress in microfabrication technology allows us to investigate experimentally the dephasing process in mesoscopic systems, for instance by observation of a particular state out of coherent superposition [6].

Although the dephasing (decoherence) plays important role in different processes, its mechanism is not elaborated enough. For instance, in many studies of the quantum measurement problems the dephasing is usually accounted for by introducing some phenomenological dissipating terms, associated with a detector (or an environment). Yet, such a procedure cannot not illuminate the origin of the dephasing and its role in the measurement problem. Most appropriate way to approach the problem, however, is to start with the microscopic description of the measured system and the detector together by use of the Schrödinger equation,  $i\dot{\sigma} = [\mathcal{H}, \sigma]$ , where  $\sigma(\mathcal{S}, \mathcal{S}'; \mathcal{D}, \mathcal{D}', t)$  is the total density-matrix and  $\mathcal{H}$  is the Hamiltonian for the entire system. Here  $\mathcal{S}(\mathcal{S}')$  and  $\mathcal{D}(\mathcal{D}')$  are the variables of the measured system and the detector respectively. In this case the influence of the detector on the measured system can be determined by “tracing out” the detector variables in the total density matrix,

$$\sum_{\mathcal{D}} \sigma(\mathcal{S}, \mathcal{S}', \mathcal{D}, \mathcal{D}, t) \rightarrow \bar{\sigma}(\mathcal{S}, \mathcal{S}', t). \quad (1.1)$$

The decoherence would correspond to an exponential damping of the off-diagonal matrix elements in the reduced density-matrix:  $\bar{\sigma}(\mathcal{S}, \mathcal{S}', t) \sim \exp(-\Gamma_d t) \rightarrow 0$  for  $\mathcal{S} \neq \mathcal{S}'$ , with  $\Gamma_d$  is the decoherence rate.

In this paper we apply the above approach to study the decoherence, generated by measurement of a quantum-dot occupancy in multi-dot systems. As the measurement device (detector) we take the ballistic point-contact in close proximity to the measured quantum dot [7]. Since the quantum-mechanical description of this detector is rather simple, it allows us to investigate the essential physics of the measurement process in great details. In addition, the ballistic point-contact is a noninvasive detector [7]. Indeed, the time which an electron

spends inside it is very short. Thus, the point-contact would not distort the measured dot. (The first measurement of decoherence in the quantum dot generated by the point-contact has been recently performed by Buks *et al.* [6]).

The plan of this paper is the following: In Sect. 2 we describe the measurement of a quantum-dot occupation, when the current flows through this dot. We use the quantum rate equations [8–12], which allow us to describe both, the measured quantum dot and the point-contact detector in the most simple way. Detailed microscopic derivation of the rate equations for the point-contact is presented in Appendix A. In Sect. 3 we investigate the decoherence of an electron in a double-well potential caused by the point-contact detector by measuring the occupation of one of the wells. Special attention is paid to comparison with the result of rapidly repeated measurement. For a description of this system we use the Bloch-type rate equations [8,9,14], which are derived in Appendix B. Similar decoherence effects, but in dc current flowing through a coupled-dot system are discussed in Sect. 4. The last section is summary.

## II. BALLISTIC POINT-CONTACT DETECTOR

Consider the measurement of electron occupation of a semiconductor quantum dot by means of a separate measuring circuit in close proximity [6,7]. A ballistic one-dimensional point-contact is used as a “detector” that resistance is very sensitive to the electrostatic field generated by an electron occupying the measured quantum dot. Such a set up is shown schematically in Fig. 1, where the detector is represented by a barrier, connected with two reservoirs at the chemical potentials  $\mu_L$  and  $\mu_R$  respectively. The transmission probability of the barrier varies from  $T$  to  $T'$ , depending on whether or not the quantum dot is occupied by an electron, Fig. 1 (a,b).

Initially all the levels in the reservoirs are filled up to the corresponding Fermi energies and the quantum dot is empty. (For simplicity we consider the reservoirs at zero temperature). Such a state is not stable, since electrons are moving from the left to the right

reservoir. The time-evolution of the entire system can be described by the master (rate) equations [8–12] (the microscopic derivation from the many-body Schrödinger equation is given in Appendix A and in Refs. [8,9]).

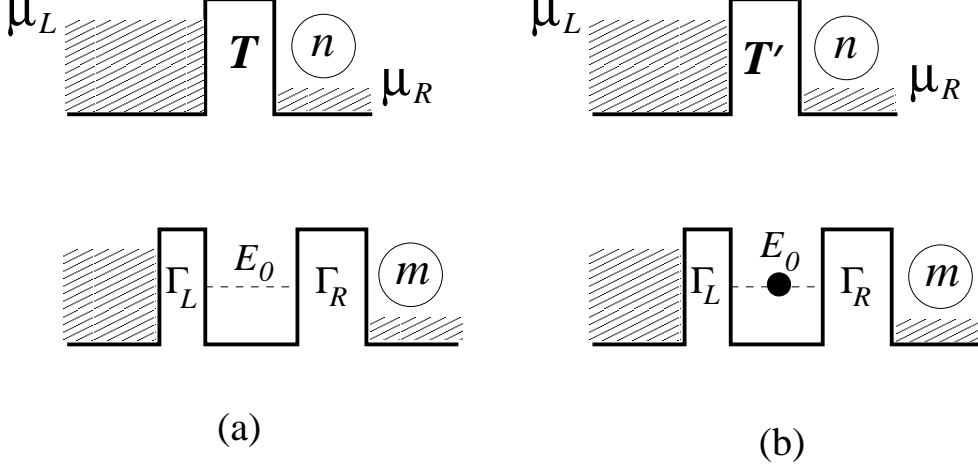


Fig. 1. Ballistic point-contact near quantum-dot.  $\Gamma_{L,R}$  are the corresponding tunneling rates. The penetration coefficient of the point-contact is  $T$  for the empty dot (a) and  $T'$  for the occupied dot (b). The indices  $m$  and  $n$  denote the number of electrons penetrating to the right reservoirs at time  $t$ .

In order to write down these equations we introduce the probabilities  $\sigma_{aa}^{m,n}(t)$  and  $\sigma_{bb}^{m,n}(t)$  of finding the entire system in the states  $|a\rangle$  and  $|b\rangle$  corresponding to empty or occupied dot (Fig. 1 a,b). Here  $m$  and  $n$  are the number of electrons penetrated to the right reservoirs of the measured system and the detector, respectively. The corresponding rate equations for these probabilities have the following form

$$\dot{\sigma}_{aa}^{m,n} = -(\Gamma_L + D)\sigma_{aa}^{m,n} + \Gamma_R\sigma_{bb}^{m-1,n} + D\sigma_{aa}^{m,n-1} \quad (2.1a)$$

$$\dot{\sigma}_{bb}^{m,n} = -(\Gamma_R + D')\sigma_{bb}^{m,n} + \Gamma_L\sigma_{aa}^{m,n} + D'\sigma_{bb}^{m,n-1}, \quad (2.1b)$$

where  $\Gamma_{L,R}$  are the transition rates for an electron tunneling from the left reservoir to the dot and from the dot to the right reservoir respectively, and  $D = T(\mu_L - \mu_R)/2\pi$  is the rate of electron hopping from the right to the left reservoir through the point-contact (the

Landauer formula).

The accumulated charge in the right reservoirs of the detector ( $d$ ) and of the measured system ( $s$ ) is given by

$$Q_d(t) = \sum_{m,n} n[\sigma_{aa}^{m,n}(t) + \sigma_{bb}^{m,n}(t)] \quad (2.2a)$$

$$Q_s(t) = \sum_{m,n} m[\sigma_{aa}^{m,n}(t) + \sigma_{bb}^{m,n}(t)] \quad (2.2b)$$

(We choose the units where the electron charge  $e = 1$ , and  $\hbar = 1$ ). The currents flowing in the detector and in the measured system are  $I_d(t) = \dot{Q}_d(t)$  and  $I_s(t) = \dot{Q}_s(t)$ . Using Eqs. (2.1) and (2.2) we obtain

$$I_d(t) = \sum_{m,n} n[\dot{\sigma}_{aa}^{m,n}(t) + \dot{\sigma}_{bb}^{m,n}(t)] = D\sigma_{aa}(t) + D'\sigma_{bb}(t), \quad (2.3a)$$

$$I_s(t) = \sum_{m,n} m[\dot{\sigma}_{aa}^{m,n}(t) + \dot{\sigma}_{bb}^{m,n}(t)] = \Gamma_R\sigma_{bb}(t), \quad (2.3b)$$

where  $\sigma_{aa} \equiv \sum_{m,n} \sigma_{aa}^{m,n}$  and  $\sigma_{bb} \equiv \sum_{m,n} \sigma_{bb}^{m,n}$  are the total probabilities of finding the dot empty or occupied. Obviously  $\sigma_{aa}(t) = 1 - \bar{\sigma}(t)$ , where  $\bar{\sigma}(t) \equiv \sigma_{bb}(t)$ . Performing the summation over  $m, n$  in Eqs. (2.1) we obtain the following rate equation for the quantum dot occupation probability  $\bar{\sigma}$

$$\dot{\bar{\sigma}}(t) = \Gamma_L - (\Gamma_L + \Gamma_R)\bar{\sigma}(t). \quad (2.4)$$

If the point-contact and the quantum dot are decoupled, the detector current is  $I_d^{(0)} = D$ . Hence, the occupation of the quantum dot can be measured through the variation of the detector current  $\Delta I_d = I_d^{(0)} - I_d$ . One readily obtains from Eq. (2.3a) that

$$\Delta I_d(t) = \frac{\Delta T V_d}{2\pi} \bar{\sigma}(t), \quad (2.5)$$

where  $V_d = \mu_L - \mu_R$  is the voltage bias, and  $\Delta T = T - T'$ . Thus, the point contact is indeed the measurement device. In fact, Eq. (2.5) is a self-evident one. Indeed, the variation of the point-contact current is  $\Delta T V_d / 2\pi$  and  $\bar{\sigma}$  is the probability for such a variation.

It follows from Eqs. (2.1), (2.3) that the same current  $I_s(t) = \Gamma_R \bar{\sigma}(t)$  would flow through the quantum dot in the absence of the detector ( $D = D' = 0$ ). It means that the point-contact detector is a noninvasive detector. This is not surprising since only an electron

inside the point-contact (under the barrier) can affect an electron in the quantum dot. The relevant (tunneling) time is very short. Actually, it is zero in the tunneling Hamiltonian approximation, Eqs. (A1), (B1), used for the derivation of the rate equations.

### III. DETECTION OF ELECTRON OSCILLATIONS IN COUPLED-DOTS

A well-known manifestation of quantum coherence is the oscillation of a particle in a double-well (double-dot) potential. The origin of these oscillations is the interference between the probability amplitudes of finding a particle in different wells. Hence, one can expect that the disclosure of a particle (electron) in one of wells would generate the “dephasing” that eventually destroys these oscillations, even without distorting the energy levels of the system.

Let us investigate the mechanism of this process by taking for detector a noninvasive point-contact. A possible set up is shown in Fig. 2.

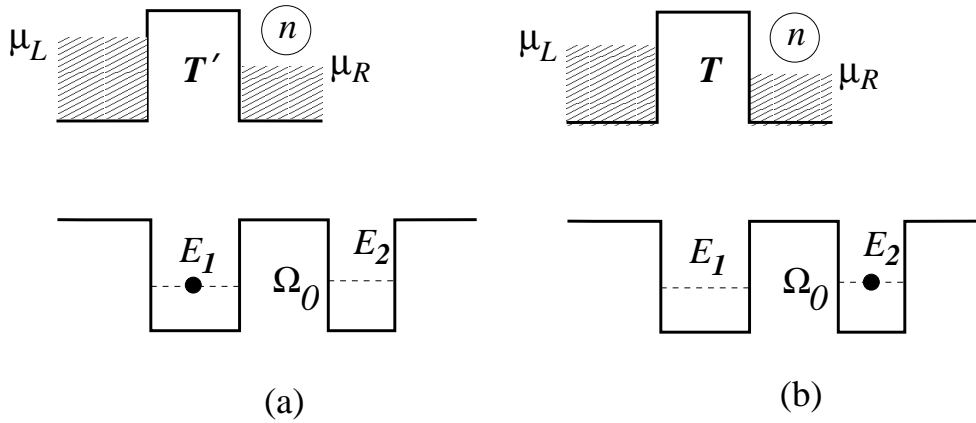


Fig. 2. Electron oscillations in the double-well. The penetration coefficient of the point-contact varies from  $T'$  to  $T$  when an electron occupies the left well (a) or the right well (b), respectively. The index  $n$  denotes the number of electrons accumulated in the collector at time  $t$ .

We assume that the transmission probability of the point-contact is  $T$  when an electron occupies the right well, and it is  $T'$  when an electron occupies the left well. Here  $T' < T$

since the right well is away from the point contact.

Now we apply the quantum-rate equations [8,9] to the whole system. However, in the distinction with the previous case, the electron transitions in the measured system take place between the *isolated* states inside the dots. As a result the diagonal density-matrix elements are coupled with the off-diagonal elements, so that the corresponding rate equations are the Bloch-type equations [8,9,14].

We first start with the case of the double-well detached from the point-contact detector. The Bloch equations describing the time evolution of the electron density-matrix  $\sigma_{ij}$  have the following form

$$\dot{\sigma}_{aa} = i\Omega_0(\sigma_{ab} - \sigma_{ba}) , \quad (3.1a)$$

$$\dot{\sigma}_{bb} = i\Omega_0(\sigma_{ba} - \sigma_{ab}) , \quad (3.1b)$$

$$\dot{\sigma}_{ab} = i\epsilon\sigma_{ab} + i\Omega_0(\sigma_{aa} - \sigma_{bb}) , \quad (3.1c)$$

where  $\epsilon = E_2 - E_1$  and  $\Omega_0$  is the coupling between the left and the right wells. Here  $\sigma_{aa}(t)$  and  $\sigma_{bb}(t)$  are the probabilities of finding the electron in the left and the right well respectively, and  $\sigma_{ab}(t) = \sigma_{ba}^*(t)$  are the off-diagonal density-matrix elements (“coherences”) [15].

Solving these equations for the initial conditions and  $\sigma_{aa}(0) = 1$  and  $\sigma_{bb}(0) = \sigma_{ab}(0) = 0$  we obtain

$$\sigma_{aa}(t) = \frac{\Omega_0^2 \cos^2(\omega t) + \epsilon^2/4}{\Omega_0^2 + \epsilon^2/4} , \quad (3.2)$$

where  $\omega = (\Omega_0^2 + \epsilon^2/4)^{1/2}$ . As expected the electron initially localized in the first well oscillates between the wells with the frequency  $\omega$ . Notice that the amplitude of these oscillations is  $\Omega_0^2/(\Omega_0^2 + \epsilon^2/4)$ . Thus the electron remains localized in the first well if the level displacement is large,  $\epsilon \gg \Omega_0$ .

Now we consider the electron oscillations in the presence of the point contact detector, Fig. 2. The corresponding Bloch equations for the entire system have the following form (Appendix B):

$$\dot{\sigma}_{aa}^n = -D'\sigma_{aa}^n + D'\sigma_{aa}^{n-1} + i\Omega_0(\sigma_{ab}^n - \sigma_{ba}^n), \quad (3.3a)$$

$$\dot{\sigma}_{bb}^n = -D\sigma_{bb}^n + D\sigma_{bb}^{n-1} - i\Omega_0(\sigma_{ab}^n - \sigma_{ba}^n), \quad (3.3b)$$

$$\dot{\sigma}_{ab}^n = i\epsilon\sigma_{ab}^n + i\Omega_0(\sigma_{aa}^n - \sigma_{bb}^n) - \frac{1}{2}(D' + D)\sigma_{ab}^n + (D D')^{1/2}\sigma_{ab}^{n-1}, \quad (3.3c)$$

Here the index  $n$  denotes the number of electrons arriving to the collector at time  $t$ , and  $D(D')$  is the transition rate of an electron hopping from the left to the right detector reservoirs,  $D = T(\mu_L - \mu_R)/2\pi$ , Eqs. (2.1). Notice that the presence of the detector results in additional terms in the rate equations in comparison with Eqs. (3.1). These terms are generated by transitions of an electron from the left to the right detector reservoirs with the rates  $D$  and  $D'$  respectively. The equation for the non-diagonal density-matrix elements  $\sigma_{ab}^n$  is slightly different from the standard Bloch equations due to the last term, which describes transition between different coherences,  $\sigma_{ab}^{n-1}$  and  $\sigma_{ab}^n$ . This term appears in the Bloch equations for coherences whenever the same hopping ( $n-1 \rightarrow n$ ) takes place in the *both* states of the off-diagonal density-matrix element ( $a$  and  $b$ ) (see Refs. [8,9] and Appendix B). The rate of such transitions is determined by a product of the corresponding *amplitudes* ( $T^{1/2}$  and  $T'^{1/2}$ ).

It follows from Eqs. (2.3a), (3.3) that the variation of the point-contact current  $\Delta I_d(t) = I^{(0)} - I_d(t)$  measures directly the charge in the first dot. Indeed, one obtains for the detector current

$$I_d(t) = \sum_n n[\sigma_{aa}^n(t) + \sigma_{bb}^n(t)] = D'\sigma_{aa}(t) + D\sigma_{bb}(t), \quad (3.4)$$

where  $\sigma_{ij} = \sum_n \sigma_{ij}^n$ . Therefore  $\Delta I_d(t)$  is given by Eq. (2.5), where  $\bar{\sigma}(t) \equiv \sigma_{aa}(t)$ .

In order to determine the influence of the detector on the double-well system we trace out the detector states in Eqs. (3.3) thus obtaining

$$\dot{\sigma}_{aa} = i\Omega_0(\sigma_{ab} - \sigma_{ba}), \quad (3.5a)$$

$$\dot{\sigma}_{bb} = i\Omega_0(\sigma_{ba} - \sigma_{ab}), \quad (3.5b)$$

$$\dot{\sigma}_{ab} = i\epsilon\sigma_{ab} + i\Omega_0(\sigma_{aa} - \sigma_{bb}) - \frac{1}{2}(\sqrt{D} - \sqrt{D'})^2\sigma_{ab}, \quad (3.5c)$$



where  $\sigma_{ij} = \sum_n \sigma_{ij}^n(t)$ .

These equations coincide with Eqs. (3.1), describing the electron oscillations without detector, except for the last term in Eq. (3.5c). The latter generates the exponential damping of the non-diagonal density-matrix element with the “dephasing” rate [16]

$$\Gamma_d = (\sqrt{D} - \sqrt{D'})^2 = (\sqrt{T} - \sqrt{T'})^2 \frac{V_d}{2\pi} \quad (3.6)$$

It implies that  $\sigma_{ab} \rightarrow 0$  for  $t \rightarrow \infty$ . We can check it by looking for the stationary solutions of Eqs. (3.5) in the limit  $t \rightarrow \infty$ . In this case  $\dot{\sigma}_{ij}(t \rightarrow \infty) = 0$  and Eqs. (3.5) become linear algebraic equations, which can be easily solved. One finds that the electron density-matrix becomes the statistical mixture.

$$\sigma(t) = \begin{pmatrix} \sigma_{aa}(t) & \sigma_{ab}(t) \\ \sigma_{ba}(t) & \sigma_{bb}(t) \end{pmatrix} \rightarrow \begin{pmatrix} 1/2 & 0 \\ 0 & 1/2 \end{pmatrix} \quad \text{for } t \rightarrow \infty. \quad (3.7)$$

Notice that the damping of the nondiagonal density matrix elements is coming entirely from the possibility of disclosing the electron in one of the wells. Indeed, if the detector does not distinguish which of the wells is occupied, i.e.  $T = T'$ , then  $\Gamma_d = 0$ .

The Bloch equations (3.3), (3.5) display explicitly the mechanism of the dephasing during a noninvasive measurement, i.e. that which does not distort the energy levels of the measured system [19]. The dephasing appears in the reduced density matrix as the “dissipative” term in the nondiagonal density matrix elements only, as a result of tracing out the detector variables. All other terms related to the detector are canceled after tracing out the detector variables. It is important to note that such a dephasing term in Eq. (3.5c) generates the “collapse” of the electron density matrix into the statistical mixture, Eq. (3.7), without explicit use of the measurement reduction postulate [20]. The collapse is fully described by the Bloch-type equations, derived from the Shrödinger equation (Appendix B).

In fact, the idea that the dissipative interaction of a measured system with a detector can be responsible for the density matrix collapse is not new. It was discussed in many publications, as for instance in works of Zurek [21], which stressed conceptual points, or in detailed studies of more specific examples of atomic transitions [22]. Yet, the present study

of mesoscopic systems elaborates additional aspects of the dephasing problem. These are the dephasing mechanism due to continuous observation with a non-invasive detector, and the striking difference between the continuous and rapidly repeated measurements. The latter is discussed below.

### A. Continuous measurement and Zeno effect

The most surprising phenomenon which displays Eq. (3.7) is that the transition to the statistical mixture takes place even for a large displacement of the energy levels,  $\epsilon \gg \Omega_0$ , irrespectively of the initial conditions. It means that an electron initially localized in one of the wells would be always *delocalized* at  $t \rightarrow \infty$ . It would happened even if the electron was initially localized at the lower level. (Of course it does not violate the energy conservation, since the double-well is not isolated). Such a behavior is not expectable because the amplitude of electron oscillations is very small for large level displacement, Eq. (3.2). Thus, the electron should stay localized in one of the wells. One could expect that the continuous observation of this electron by a detector could only increase its localization. It can be inferred from so called Zeno effect [23]. The latter tells us that repeated observation of the system slow down transitions between quantum states due to the collapse of the wave function into the observed state. Since in our case the change of the detector current,  $\Delta I_s(t)$  monitors  $\bar{\sigma}(t)$  in the left well, Eq. (2.5), (3.4), it represents the continuous measurement of the charge in this well. Nevertheless the effects is just opposite – the continuous measurement delocalizes the system [24].

In fact, our results for small  $t$  seems to be in an agreement with the Zeno effect, even so we have not explicitly implied the projection postulate. For instance, Fig. 3a shows the time-dependence of the probability to find an electron in the left dot, as obtained from the solution of Eqs. (3.5) for the aligned levels ( $\epsilon = 0$ ), and  $\Gamma_d = 0$  (dashed curve),  $\Gamma_d = 4\Omega_0$  (dot-dashed curve) and  $\Gamma_d = 16\Omega_0$  (solid curve). One finds that for small  $t$  the rate of transition from the left to the right well decreases with the increase of  $\Gamma_d$ .

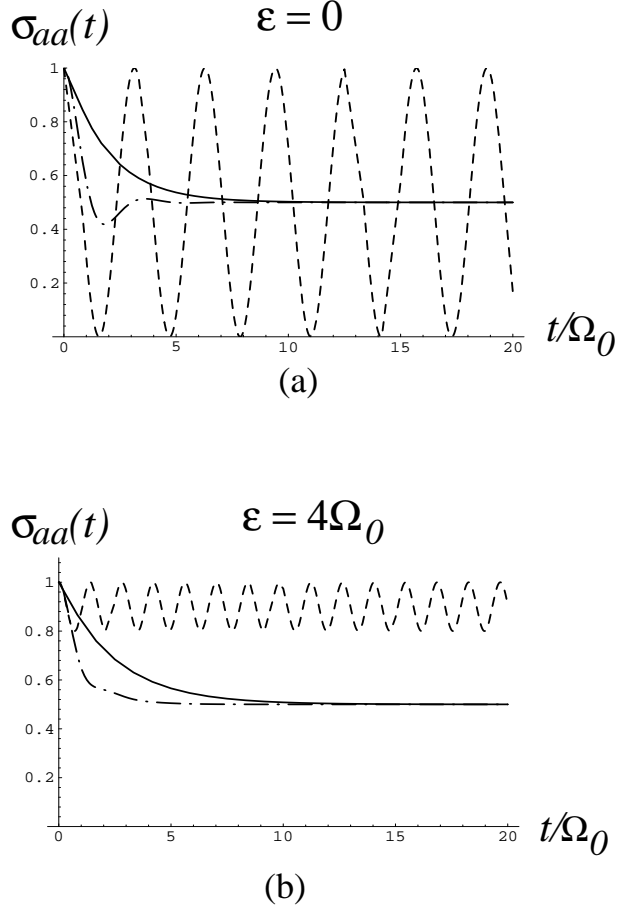


Fig. 3. The occupation of the first well as a function of time, Eqs. (3.5): (a) the levels are aligned ( $\epsilon = 0$ ); (b) the levels are displaced ( $\epsilon = 4\Omega_0$ ). The curves correspond to different values of the dephasing rate:  $\Gamma_d = 0$  (dashed),  $\Gamma_d = 4\Omega_0$  (dot-dashed), and  $\Gamma_d = 16\Omega_0$  (solid).

The same slowing down of the transition rate for small  $t$  we find for the disaligned levels ( $\epsilon = 4\Omega_0$ ) in Fig. 3b. It implies that very frequent repeated measurements would indeed localize the system. In that sense the Bloch equations reproduce the Zeno effect without explicit use of the projection postulate. Actually, this result has been found earlier by an analysis of atomic transitions by using the Bloch equation for 3-level system [25,26]. It was shown that the repeated measurement with short intervals  $\Delta t = t/n$  localizes the system

in the limit  $n \rightarrow \infty$ . Yet in our case the continuous measurement leads to an electron *delocalization*, whereas in the absence of detector an electron would stay localized in the left well (the dashed curve in Fig. 3b). Thus the continuous and very frequent repeated measurements affect the system in opposite ways.

Our microscopic treatment allows us to determine the origin of the difference in both treatments. One easily finds that the derivation of the Bloch-type of equations, describing the measured system, Eqs. (3.5) implies the tracing of the detector variables, Eq. (1.1). Since this procedure is outside the Schrödinger equation, it could distort the time development of the system. In our case of continuous measurement the tracing is done at the time  $t$ , whereas the frequent repeated measurement with the intervals  $\Delta t = t/n$  implies that the tracing of the detector variables takes part at the end of each interval  $\Delta t$ . As a result the limit of  $n \rightarrow \infty$  the measured system stays localized [25].

#### IV. MEASUREMENT OF RESONANT CURRENT IN COUPLED-DOTS

In spite of great progress made in the microfabrication technique, the direct measurement of single electron oscillations in coupled-dot system is still a complicated problem. However, it is much easier to measure similar quantum coherence effects in electrical current flowing through coupled-dot systems. We therefore consider the same coupled-dot of the previous section, but now connected with two reservoirs (emitter and collector). As in the previous example the point-contact detector measures the occupation of the left dot, Fig. 4. For the sake of simplicity we assume strong inner and inter-dot Coulomb repulsion, so only one electron can occupy this system [14]. Then there are only three available states of the coupled-dot system: the dots are empty (*a*), the first dot is occupied (*b*) and the second dot is occupied (*c*). In an analogy with Eqs. (2.1), (3.3) we write the following Bloch equations for the density matrix  $\sigma_{ij}^{m,n}(t)$  describing the entire system [8,9]:

$$\dot{\sigma}_{aa}^{m,n} = -(\Gamma_L + D)\sigma_{aa}^{m,n} + \Gamma_R\sigma_{cc}^{m-1,n} + D\sigma_{aa}^{m,n-1}, \quad (4.1a)$$

$$\dot{\sigma}_{bb}^{m,n} = -D'\sigma_{bb}^{m,n} + D'\sigma_{bb}^{m,n-1} + \Gamma_L\sigma_{aa}^{m,n} + i\Omega_0(\sigma_{bc}^{m,n} - \sigma_{cb}^{m,n}), \quad (4.1b)$$

$$\dot{\sigma}_{cc}^{m,n} = -(\Gamma_R + D)\sigma_{cc}^{m,n} + D\sigma_{cc}^{m,n-1} - i\Omega_0(\sigma_{bc}^{m,n} - \sigma_{cb}^{m,n}), \quad (4.1c)$$

$$\dot{\sigma}_{bc}^{m,n} = i\epsilon\sigma_{bc}^{m,n} + i\Omega_0(\sigma_{bb}^{m,n} - \sigma_{cc}^{m,n}) - \frac{1}{2}(\Gamma_R + D' + D)\sigma_{bc}^{m,n} + (D D')^{1/2}\sigma_{bc}^{m,n-1}, \quad (4.1d)$$

where the indices  $n$  and  $m$  denote the number of electrons arrived at time  $t$  to the upper and the lower collector reservoir, respectively. Here  $\Gamma_L$ ,  $\Gamma_R$  are the rates of electron transitions from the left reservoir to the first dot and from the second dot to the right reservoir, and  $\Omega_0$  is the amplitude of hopping between two dots.

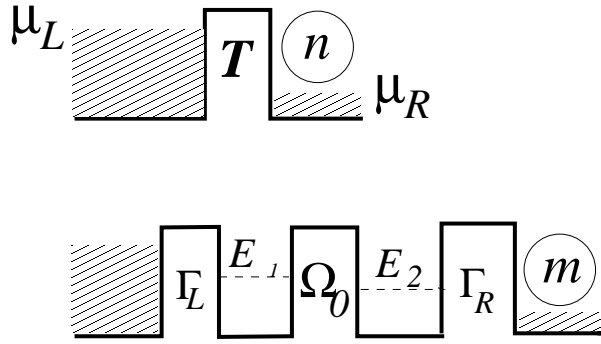


Fig. 4. Resonant tunneling through the double-dot.  $\Gamma_{L,R}$  denote the corresponding rate for the tunneling from (to) the left (right) reservoirs. The penetration coefficient of the point-contact is  $T$  for the empty double-dot system or for the occupied second dot, and it is  $T'$  for the occupied first dot. The indices  $m$  and  $n$  denote the number of electrons penetrating to the right reservoirs at time  $t$ .

The currents in the double-dot system ( $I_s$ ) and in the detector ( $I_d$ ) are given by the following expressions (c.f. Eqs. (2.2), (2.3b)):

$$I_s = \sum_{m,n} m(\dot{\sigma}_{aa}^{m,n} + \dot{\sigma}_{bb}^{m,n} + \dot{\sigma}_{cc}^{m,n}) = \Gamma_R \sigma_{cc} \quad (4.2a)$$

$$I_d = \sum_{m,n} n(\dot{\sigma}_{aa}^{m,n} + \dot{\sigma}_{bb}^{m,n} + \dot{\sigma}_{cc}^{m,n}) = D - (D - D')\sigma_{bb} \quad (4.2b)$$

where  $\sigma_{ij} = \sum_{m,n} \sigma_{ij}^{m,n}$ . It follows from Eq. (4.2b) that the variation of the detector current  $\Delta I_d = I_d^{(0)} - I_d$  is given by Eq. (2.5), where  $\bar{\sigma} = \sigma_{bb}$ . Thus, the point-contact measures

directly the occupation of the left dot.

Performing summation in Eqs. (4.1) over the number of electrons arrived to the collectors  $(m, n)$ , we obtain the following Bloch equations for the reduced density-matrix of the double-dot system:

$$\dot{\sigma}_{aa} = -\Gamma_L \sigma_{aa} + \Gamma_R \sigma_{cc} \quad (4.3a)$$

$$\dot{\sigma}_{bb} = \Gamma_L \sigma_{aa} + i\Omega_0(\sigma_{bc} - \sigma_{cb}) \quad (4.3b)$$

$$\dot{\sigma}_{cc} = -\Gamma_R \sigma_{cc} - i\Omega_0(\sigma_{bc} - \sigma_{cb}) \quad (4.3c)$$

$$\dot{\sigma}_{bc} = i\epsilon \sigma_{bc} + i\Omega_0(\sigma_{bb} - \sigma_{cc}) - \frac{1}{2}(\Gamma_R + \Gamma_d)\sigma_{bc}, \quad (4.3d)$$

where  $\Gamma_d$  is the dephasing rate generated by the detector, Eq. (3.6). These equations can be compared with those describing electron transport through the same system, but without detector [8,9,14]. We find that the difference appears only in the nondiagonal density-matrix elements, Eq. (4.3d). The latter includes an additional dissipation rate  $\Gamma_d$  generated by the detector.

Solving Eqs. (4.3) in the limit  $t \rightarrow \infty$  we find the following expression for the current  $I_s$ , Eq. (4.2b), flowing through the double-dot system

$$I_s = \frac{(\Gamma_R + \Gamma_d)\Omega_0^2}{\epsilon^2 + \frac{(\Gamma_R + \Gamma_d)^2}{4} + \Omega_0^2(\Gamma_R + \Gamma_d) \left( \frac{2}{\Gamma_R} + \frac{1}{\Gamma_L} \right)} \quad (4.4)$$

By analyzing Eq. (4.4) one finds that all the measurement effects, discussed in the previous section are reflected in the behavior of the resonant current,  $I_s$  as a function of the level displacement  $\epsilon$  and the dephasing rate  $\Gamma_d$ . As an example, we show in Fig. 5 the resonant current  $I_s(\epsilon)$  for three values of the dephasing rate:  $\Gamma_d = 0$ ,  $\Gamma_d = 4\Omega_0$  and  $\Gamma_d = 16\Omega_0$ . We find that for small  $\epsilon$  the current decreases with  $\Gamma_d$ , while for large  $t$  the average distribution of an electron in the dots remains the same. However, for larger values of  $\epsilon$  the current *increases* with  $\Gamma_d$ . It reflects electron delocalization in a double-well system, Fig. 3b, due to continuous monitoring of the charge in the left dot. In contrast, rapidly repeated measurement [22,25] would always localize an electron and therefore diminish the current  $I_s$ .

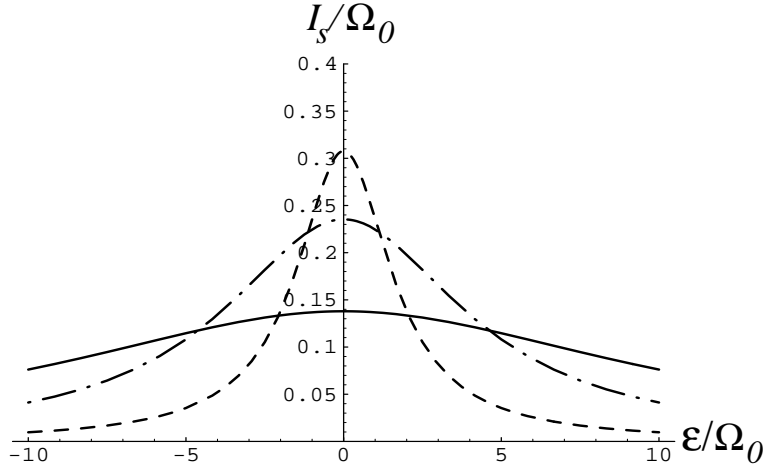


Fig. 5. Electron current through the doubled-dot, Eq. (4.4), for  $\Gamma_L = \Gamma_R = \Omega_0$  as a function of the level displacement  $\epsilon = E_2 - E_1$ . The curves correspond to different values of the dephasing rate:  $\Gamma_d = 0$  (dashed),  $\Gamma_d = 4\Omega_0$  (dot-dashed) and  $\Gamma_d = 16\Omega_0$  (solid).

## V. SUMMARY

In this paper we studied the mechanism of decoherence generated by continuous observation of one of the states out of the coherent superposition in experiments with mesoscopic systems. As an example we considered a coupled quantum-dot system, which is simple enough for detailed theoretical treatment of the measured object and the detector together. On the other hand, it bears all essential physics of the measurement process. For a description of the entire system we applied the Bloch-type equations, which are obtained from the many-body Schrödinger equation and provide the most simple and transparent treatment of quantum coherence effects.

As the detector we used the point contact in close proximity to one of the dots. We

demonstrated that the variation of the point-contact current due to electrostatic interaction with electrons in the dot measures directly the occupation of this dot.

We started with quantum oscillations of an electron in coupled quantum dots. It appears that the presence of the point-contact detector near one of the dots generates the dephasing rate in the Bloch equations for the off-diagonal density matrix elements. We found that the dephasing rate is proportional to the variation of the point-contact transmission amplitude squared, Eq (3.6). The Bloch equations for the diagonal density-matrix elements are not affected by the detector, providing that it does not distort the energy levels of the double-dot system.

The appearance of the dephasing rate  $\Gamma_d$  in the Bloch equation leads to the collapse of the density matrix into the statistical mixture at  $t \rightarrow \infty$ , Eq. (3.7). The collapse happens even for large disalignment of the energy levels. In this case the measurement process results in an electron delocalization inside the double-dot (after some critical time  $t > t_0$ ), which otherwise would stay localized in one of the dots. It contradicts to a common opinion that the continuous measurement always leads to a localization due to the wave-packet reduction (Zeno effect). In fact the localization would take place if we consider the continuous measurement as rapidly repeated measurements with intervals  $\Delta t = t/n$  for  $n \rightarrow \infty$ . The reason of such a different behavior of the measured system stems from the different procedure of tracing out of the detector variables from the total density matrix.

The same measurement effects appear in the dc current flowing through coupled-dots. We found that the dc current vanishes for  $\Gamma_d \rightarrow \infty$ , which can be interpreted in terms of an electron localization due to the Zeno effect. Nevertheless, for a finite  $\Gamma_d$  and for a disaligned energy levels ( $E_1 \neq E_2$ ) the dc current *increases* with  $\Gamma_d$ . Here again, the situation is opposite to that of rapidly repeated measurement, where the current always *decreases* with  $\Gamma_d$ .



## VI. ACKNOWLEDGMENTS

I owe special thanks to E. Buks for fruitful discussions on various theoretical and experimental aspects. I am also grateful to M. Heiblum and Y. Levinson for useful discussions.

## APPENDIX A: RATE EQUATIONS FOR A POINT-CONTACT DETECTOR

We present here the microscopic derivation of the rate equations describing electron transport in the point contact. The point-contact is considered as a barrier, separated two reservoirs (the emitter and the collector), Fig. 1. All the levels in the emitter and the collector are initially filled up to the Fermi energies  $\mu_L$  and  $\mu_R$  respectively. We call it as the “vacuum” state,  $|0\rangle$ . The tunneling Hamiltonian  $\mathcal{H}_{pc}$  describing this system can be written as

$$\mathcal{H}_{PC} = \sum_l E_l a_l^\dagger a_l + \sum_r E_r a_r^\dagger a_r + \sum_{l,r} \Omega_{lr} (a_l^\dagger a_r + H.c.), \quad (A1)$$

where  $a_l^\dagger(a_l)$  and  $a_r^\dagger(a_r)$  are the creation (annihilation) operators in the left and the right reservoirs, respectively, and  $\Omega_{lr}$  is the hopping amplitude between the states  $E_l$  and  $E_r$  in the right and the left reservoirs. (We choose the gauge where  $\Omega_{lr}$  is real). The Hamiltonian Eq. (A1) requires the vacuum state  $|0\rangle$  to decay exponentially to a continuum states having the form:  $a_r^\dagger a_l |0\rangle$  with an electron in the collector continuum and a hole in the emitter continuum;  $a_r^\dagger a_{r'}^\dagger a_l^\dagger a_{l'} |0\rangle$  with two electrons in the collector continuum and two holes in the emitter continuum, and so on. The many-body wave function describing this system can be written in the occupation number representation as

$$|\Psi(t)\rangle = \left[ b_0(t) + \sum_{l,r} b_{lr}(t) a_r^\dagger a_l + \sum_{l<l',r<r'} b_{ll'rr'}(t) a_r^\dagger a_{r'}^\dagger a_l a_{l'} + \dots \right] |0\rangle, \quad (A2)$$

where  $b(t)$  are the time-dependent probability amplitudes to find the system in the corresponding states with the initial condition  $b_0(0) = 1$ , and all the other  $b(0)$ ’s being zeros. Substituting Eq. (A2) into the Shrödinger equation  $i\dot{|\Psi(t)\rangle} = \mathcal{H}_{PC}|\Psi(t)\rangle$  and performing the Laplace transform,

$$\tilde{b}(E) = \int_0^\infty e^{iEt} b(t) dt \quad (\text{A3})$$

we obtain an infinite set of the coupled equations for the amplitudes  $\tilde{b}(E)$ :

$$E\tilde{b}_0(E) - \sum_{l,r} \Omega_{lr} \tilde{b}_{lr}(E) = i \quad (\text{A4a})$$

$$(E + E_l - E_r) \tilde{b}_{lr}(E) - \Omega_{lr} \tilde{b}_0(E) - \sum_{l',r'} \Omega_{l'r'} \tilde{b}_{ll'rr'}(E) = 0 \quad (\text{A4b})$$

$$(E + E_l + E_{l'} - E_r - E_{r'}) \tilde{b}_{ll'rr'}(E) - \Omega_{l'r'} \tilde{b}_{lr}(E) + \Omega_{lr} \tilde{b}_{l'r'}(E) - \sum_{l'',r''} \Omega_{l''r''} \tilde{b}_{ll'l''rr'r''}(E) = 0 \quad (\text{A4c})$$

.....

Eqs. (A4) can be substantially simplified by replacing the amplitude  $\tilde{b}$  in the term  $\sum \Omega \tilde{b}$  of each of the equations by its expression obtained from the subsequent equation [8,9]. For example, substituting  $\tilde{b}_{lr}(E)$  from Eq. (A4b) into Eq. (A4a), one obtains

$$\left[ E - \sum_{l,r} \frac{\Omega^2}{E + E_l - E_r} \right] \tilde{b}_0(E) - \sum_{ll',rr'} \frac{\Omega^2}{E + E_l - E_r} \tilde{b}_{ll'rr'}(E) = i, \quad (\text{A5})$$

where we assumed that the hopping amplitudes are weakly dependent functions on the energies  $\Omega_{lr} \equiv \Omega(E_l, E_r) = \Omega$ . Since the states in the reservoirs are very dense (continuum), one can replace the sums over  $l$  and  $r$  by integrals, for instance  $\sum_{l,r} \rightarrow \int \rho_L(E_l) \rho_R(E_r) dE_l dE_r$ , where  $\rho_{L,R}$  are the density of states in the emitter and collector. Then the first sum in Eq. (A5) becomes an integral which can be split into a sum of the singular and principal value parts. The singular part yields  $i\pi\Omega^2\rho_L\rho_R V_d$ , and the principal part is merely included into redefinition of the energy levels. The second sum in Eq. (A5) can be neglected. Indeed, by replacing  $\tilde{b}_{ll'rr'}(E) \equiv \tilde{b}(E, E_l, E_{l'}, E_r, E_{r'})$  and the sums by the integrals we find that the integrand has the poles on the same sides of the integration contours. It means that the corresponding integral vanishes, providing  $V_d \gg \Omega^2\rho$ .

Applying analogous considerations to the other equations of the system (A4), we finally arrive to the following set of equations:

$$(E + iD/2) \tilde{b}_0 = i \quad (\text{A6a})$$

$$(E + E_l - E_r + iD/2)\tilde{b}_{lr} - \Omega\tilde{b}_0 = 0 \quad (\text{A6b})$$

$$(E + E_l + E_{l'} - E_r - E_{r'} + iD/2)\tilde{b}_{ll'rr'} - \Omega\tilde{b}_{lr} + \Omega\tilde{b}_{l'r'} = 0, \quad (\text{A6c})$$

.....

where  $D = 2\pi\Omega^2\rho_L\rho_R V_d$ .

The charge accumulated in the collector at time  $t$  is

$$N_R(t) = \langle \Psi(t) | \sum_r a_r^\dagger a_r | \Psi(t) \rangle = \sum_n n \sigma^{(n)}(t), \quad (\text{A7})$$

where

$$\sigma^{(0)}(t) = |b_0(t)|^2, \quad \sigma^{(1)}(t) = \sum_{l,r} |b_{lr}(t)|^2, \quad \sigma^{(2)}(t) = \sum_{ll',rr'} |b_{ll'rr'}(t)|^2, \quad \dots \quad (\text{A8})$$

are the probabilities to find  $n$  electrons in the collector. These probabilities are directly related to the amplitudes  $\tilde{b}(E)$  through the inverse Laplace transform

$$\sigma^{(n)}(t) = \sum_{l,\dots,r,\dots} \int \frac{dE dE'}{4\pi^2} \tilde{b}_{l,\dots,r,\dots}(E) \tilde{b}_{l,\dots,r,\dots}^*(E') e^{i(E'-E)t} \quad (\text{A9})$$

Using Eq. (A9) one can transform Eqs. (A6) into the rate equations for  $\sigma^{(n)}(t)$  (c.f. [8,9]).

We find

$$\dot{\sigma}^{(0)}(t) = -D\sigma^{(0)}(t) \quad (\text{A10a})$$

$$\dot{\sigma}^{(1)}(t) = D\sigma^{(0)}(t) - D\sigma^{(1)}(t) \quad (\text{A10b})$$

$$\dot{\sigma}^{(2)}(t) = D\sigma^{(1)}(t) - D\sigma^{(2)}(t) \quad (\text{A10c})$$

.....

The operator, which defines the current flowing in this system is

$$\hat{I} = i \left[ \mathcal{H}_{PC}, \sum_r a_r^\dagger a_r \right] = i \sum_{l,r} \Omega_{lr} (a_l^\dagger a_r - a_r^\dagger a_l) \quad (\text{A11})$$

Using Eqs. (A2), (A10) and (A11) we find for the current

$$I = \langle \Psi(t) | \hat{I} | \Psi(t) \rangle = D \sum_n \sigma^{(n)}(t) = D. \quad (\text{A12})$$

Since  $D = (2\pi)^2 \Omega^2 \rho_L \rho_R = T$  [27], where  $T$  is the transmission probability, the current can be rewritten as  $I = T V_d / (2\pi)$ , which is the well known Landauer formula.

## APPENDIX B: POINT-CONTACT DETECTOR NEAR DOUBLE-WELL

Now we present the microscopic derivation of the Bloch equations (3.3) describing electron oscillations in a double-well with a point-contact in close proximity to one of the wells, Fig. 2. We start with the many-body Schrödinger equation  $i|\dot{\Psi}(t)\rangle = \mathcal{H}|\Psi(t)\rangle$  for the entire system. Here  $\mathcal{H}$  is the tunneling Hamiltonian, which can be written as  $\mathcal{H} = \mathcal{H}_{PC} + \mathcal{H}_{DD} + \mathcal{H}_{int}$ . Here  $\mathcal{H}_{PC}$  is the tunneling Hamiltonian for the point-contact detector, Eq. (A1);  $\mathcal{H}_{DD}$  is tunneling Hamiltonian for the measured double-dot system,

$$\mathcal{H}_{DD} = E_1 c_1^\dagger c_1 + E_2 c_2^\dagger c_2 + \Omega_0 (c_2^\dagger c_1 + c_1^\dagger c_2), \quad (\text{B1})$$

and  $\mathcal{H}_{int}$  describes the interaction between the detector and the measured system. Since the presence of an electron in the left well results in an effective increase of the point-contact barrier ( $\Omega_{lr} \rightarrow \Omega_{lr} + \delta\Omega_{lr}$ ), we can represent the interaction term as

$$\mathcal{H}_{int} = \sum_{l,r} \delta\Omega_{lr} c_1^\dagger c_1 (a_l^\dagger a_r + H.c.). \quad (\text{B2})$$

The many-body wave function for the entire system can be written as

$$|\Psi(t)\rangle = \left[ b_1(t) c_1^\dagger + \sum_{l,r} b_{1lr}(t) c_1^\dagger a_r^\dagger a_l + \sum_{l < l', r < r'} b_{1ll'rr'}(t) c_1^\dagger a_r^\dagger a_{r'}^\dagger a_l a_{l'} + b_2(t) c_2^\dagger + \sum_{l,r} b_{2lr}(t) c_2^\dagger a_r^\dagger a_l + \sum_{l < l', r < r'} b_{2ll'rr'}(t) c_2^\dagger a_r^\dagger a_{r'}^\dagger a_l a_{l'} + \dots \right] |0\rangle, \quad (\text{B3})$$

where  $b(t)$  are the probability amplitudes to find the entire system in the states defined by the corresponding creation and annihilation operators. Notice that Eq. (B3) has the same form as Eq. (A2), where only the probability amplitudes  $b(t)$  acquire an additional index ('1' or '2') that denotes the well, occupied by an electron. Proceeding in the same way as in Appendix A we arrive to an infinite set of the coupled equations for the amplitudes  $\tilde{b}(E)$ , which are the Laplace transform of the amplitudes  $b(t)$ , Eq. (A3):

$$(E - E_1) \tilde{b}_1(E) - \Omega_0 \tilde{b}_2(E) - \sum_{l,r} \Omega'_{lr} \tilde{b}_{1lr}(E) = i \quad (\text{B4a})$$

$$(E - E_2) \tilde{b}_2(E) - \Omega_0 \tilde{b}_1(E) - \sum_{l,r} \Omega_{lr} \tilde{b}_{2lr}(E) = 0 \quad (\text{B4b})$$

$$(E + E_l - E_1 - E_r)\tilde{b}_{1lr}(E) - \Omega'_{lr}\tilde{b}_1(E) - \Omega_0\tilde{b}_{2lr}(E) - \sum_{l',r'}\Omega_{l'r'}\tilde{b}_{1l'r'r'}(E) = 0 \quad (\text{B4c})$$

$$(E + E_l - E_2 - E_r)\tilde{b}_{2lr}(E) - \Omega_{lr}\tilde{b}_2(E) - \Omega_0\tilde{b}_{1lr}(E) - \sum_{l',r'}\Omega_{l'r'}\tilde{b}_{2l'r'r'}(E) = 0 \quad (\text{B4d})$$

.....

The same algebra as that used in the Appendix A and in Refs. [8,9] allows us to simplify these equations, which then become

$$(E - E_1 + iD'/2)\tilde{b}_1 - \Omega_0\tilde{b}_2 = i \quad (\text{B5a})$$

$$(E - E_2 + iD/2)\tilde{b}_2 - \Omega_0\tilde{b}_1 = 0 \quad (\text{B5b})$$

$$(E + E_l - E_1 - E_r + iD'/2)\tilde{b}_{1lr} - \Omega'_{lr}\tilde{b}_1 - \Omega_0\tilde{b}_{2lr} = 0 \quad (\text{B5c})$$

$$(E + E_l - E_2 - E_r + iD/2)\tilde{b}_{2lr} - \Omega_{lr}\tilde{b}_2 - \Omega_0\tilde{b}_{1lr} = 0 \quad (\text{B5d})$$

.....

where  $D = TV_d/2\pi$ . (We assumed for simplicity that the hopping amplitude of the point-contact is weakly dependent on the energies, so that  $\Omega_{lr} \equiv \Omega(E_l, E_r) = \Omega$ ).

Using the inverse Laplace transform (A9) we can transform Eqs. (B5) into differential equations for the density-matrix elements  $\sigma_{ij}^{(n)}(t)$  ( $i, j=1,2$ )

$$\sigma_{ij}^{(0)}(t) = b_i(t)b_j^*(t), \quad \sigma_{ij}^{(1)}(t) = \sum_{l,r} b_{ilr}(t)b_{jl}^*(t), \quad \sigma_{ij}^{(2)}(t) = \sum_{l'l',rr'} b_{ill'r'r'}(t)b_{jll'r'r'}^*(t), \quad \dots, \quad (\text{B6})$$

where  $n$  denotes the number of electrons accumulated in the collector. Consider, for instance the off-diagonal density-matrix element  $\sigma_{12}^{(1)}(t)$ . The corresponding differential equation for this term can be obtained by multiplying Eq. (B5c) by  $\tilde{b}_{2lr}^*(E')$  and subtracting the complex conjugated Eq. (B5d) multiplied by  $\tilde{b}_{1lr}(E)$ . We then obtain

$$\begin{aligned} \int \frac{dE dE'}{4\pi^2} \sum_{l,r} \left\{ \left( E' - E - \epsilon - i\frac{D+D'}{2} \right) \tilde{b}_{1lr}(E)\tilde{b}_{2lr}^*(E') \right. \\ \left. - [\Omega\tilde{b}_{1lr}(E)\tilde{b}_2^*(E') - \Omega'_{lr}\tilde{b}_2^*(E')\tilde{b}_1(E)] \right. \\ \left. - \Omega_0[\tilde{b}_{1lr}(E)\tilde{b}_{1lr}^*(E') - \tilde{b}_{2lr}^*(E')\tilde{b}_{2lr}(E)] \right\} e^{i(E'-E)t} = 0. \quad (\text{B7}) \end{aligned}$$

One easily finds that the first term in this equation equals to  $-i\dot{\sigma}_{12}^{(1)} - [\epsilon + i(D+D')/2]\sigma_{12}^{(1)}$  and the third term equals to  $-\Omega_0(\sigma_{11}^{(1)} - \sigma_{22}^{(1)})$ . In order to evaluate the second term in Eq. (B7) we replace  $\sum_{l,r}$  by the integrals and substitute

$$\begin{aligned}
\tilde{b}_{1lr}(E) &= \frac{\Omega' \tilde{b}_1(E) + \Omega_0 \tilde{b}_{2lr}(E)}{E + E_l - E_1 - E_r + iD'/2} \\
\tilde{b}_{2lr}^*(E') &= \frac{\Omega \tilde{b}_2^*(E') + \Omega_0 \tilde{b}_{1lr}^*(E')}{E' + E_l - E_2 - E_r - iD/2}
\end{aligned} \tag{B8}$$

obtained from Eqs. (B5c), (B5d), into Eq. (B7). Then integrating over  $E_l, E_r$  we find that the second term in Eq. (B7) becomes  $2i\pi\Omega\Omega'\rho_L\rho_R V_d \sigma_{12}^{(0)}$ . Thus Eq. (B7) can be rewritten as

$$\dot{\sigma}_{12}^{(1)} = i\epsilon\sigma_{12}^{(1)} + i\Omega_0(\sigma_{11}^{(1)} - \sigma_{22}^{(1)}) - \frac{1}{2}(D' + D)\sigma_{12}^{(1)} + (D D')^{1/2}\sigma_{12}^{(0)}. \tag{B9}$$

which coincides with the Bloch equation (3.3c) for  $n = 1$  and  $\sigma_{aa} \equiv \sigma_{11}$ ,  $\sigma_{bb} \equiv \sigma_{22}$ ,  $\sigma_{ab} \equiv \sigma_{12}$ . Applying the same procedure to each of the equations (B5) we arrive to the Bloch equations (3.3) for density matrix elements  $\sigma_{ij}^{(n)}$ .

## REFERENCES

- [1] A.Yacoby, M. Heiblum, V. Umansky, H. Shtrikman and D. Mahalu, Phys. Rev. Lett. **73**, 3149 (1994).
- [2] R. Shuster, E. Buks, M. Heiblum, D. Mahalu, V. Umansky and H. Shtrikman, Nature, **385**, 417 (1997).
- [3] A.Yacoby, M. Heiblum, V. Umansky, H. Shtrikman and D. Mahalu, Phys. Rev. Lett. **74**, 4047 (1995).
- [4] E. Buks, R. Shuster, M. Heiblum, D. Mahalu, V. Umansky and H. Shtrikman, Phys. Rev. Lett. **77**, 4664 (1996).
- [5] N.C. van der Vaart, S.F. Godijn, Y.V. Nazarov, C.J.P.M. Hartmans, J.E. Mooij, L.W. Molenkamp, and C.T. Foxon, Phys. Rev. Lett. **74**, 4702 (1995).
- [6] E. Buks, R. Shuster, M. Heiblum, D. Mahalu, V. Umansky and H. Shtrikman, Bulletin of the American Physical Society, **42**(1), 769 (1997).
- [7] M. Field *et al.*, Phys. Rev. Lett. **70**, 1311 (1993).
- [8] S.A. Gurvitz and Ya.S. Prager, Phys. Rev. B **53**, 15932 (1996).
- [9] S.A. Gurvitz, cond-mat/9702071.
- [10] L.I. Glazman and K.A. Matveev, Pis'ma Zh. Eksp. Teor. Fiz. **48**, 403 (1988) [JETP Lett. **48**, 445 (1988)].
- [11] D.V. Averin and A.N. Korotkov, Zh. Eksp. Teor. Fiz. **97**, 1661 (1990) [Sov. Phys.–JETP **70**, 937 (1990)].
- [12] C.W.J. Beenakker, Phys. Rev. B **44**, 1646 (1991).
- [13] S.A. Gurvitz, quant-ph/9603007.
- [14] Yu.V. Nazarov, Physica B **189**, 57 (1993), T.H. Stoof and Yu.V. Nazarov, Phys. Rev.

- B **55**, 1050 (1996).
- [15] C. Cohen-Tannoudji, J. Dupont-Roc, and G. Grynberg, *Atom-Photon Interactions: Basic Processes and Applications* (Wiley, New York, 1992).
  - [16] Note that  $\Gamma_d \simeq (\Delta T)^2 V_d / 8\pi T$  for  $\Delta T \ll T$ , where  $\Delta T = T - T'$ . It is different from a similar expression for the dephasing rate found in [17,18] by a factor  $(1 - T)$ .
  - [17] I.L. Aleiner, N.S. Wingreen, and Y. Meir, cond-mat/9702001.
  - [18] Y. Levinson, Europhys. Lett. **39**, 299 (1997).
  - [19] In fact, the level distortion alone cannot totally destroy quantum oscillations. Indeed, the mismatch of the energy levels in a double-well potential ( $\epsilon \neq 0$ ) does only diminish the amplitude of quantum oscillations.
  - [20] J. von Neumann, *Mathematische Grundlagen der Quantentheorie* (Springer, Berlin, 1931).
  - [21] W.H. Zurek, Physics Today **44**, No. 10, 36 (1991); *ibid*, **46**, No. 4, 13 (1993).
  - [22] A. Beige and G.C Hegerfeldt, Phys. Rev. A**53**, 51 (1996); W.L. Power and P.L. Knight, Phys. Rev. A**53**, 1052 (1996), and references therein.
  - [23] B. Misra and E.C.G. Sudarshan, J. Math. Phys. **18**, 756 (1977); C. Presilla, R. Onofrio and U. Tambini, Ann. of Phys. **248**, 95 (1996), and references therein.
  - [24] Notice that the previous investigations of the Zeno effect in atomic system [22,25] always considered the situation corresponding to alignment levels ( $E_1 = E_2$ ) in our case. As a result the average probability of finding an electron on one of the levels remains the same before and after the density-matrix collapse.
  - [25] E. Block and P.R. Berman, Phys. Rev. A**44**, 1466 (1991); V. Frerichs and A. Schenzle, Phys. Rev. A**44**, 1962 (1991).



- [26] Notice, that our Bloch-type equations (3.3), (3.5) cannot be mapped to the Bloch equations for 3-level system [25] due to continuum-to-continuum transitions in the point-contact detector.
- [27] J. Bardeen, Phys. Rev. Lett., **6**, 57 (1961).